

Received November 26, 2020, accepted December 21, 2020, date of publication December 24, 2020, date of current version January 5, 2021.

Digital Object Identifier 10.1109/ACCESS.2020.3047158

On the Performance of the Two-Diode Model for Photovoltaic Cells Under Indoor Artificial Lighting

XINYU MA^{ID}, (Student Member, IEEE), SEBASTIAN BADER^{ID}, (Senior Member, IEEE),
AND BENGT OELMANN^{ID}

Department of Electronics Design, Mid Sweden University, SE-85170 Sundsvall, Sweden

Corresponding author: Sebastian Bader (sebastian.bader@miun.se)

ABSTRACT Models of photovoltaic devices are an important tool for the estimation of their I-V characteristics. These characteristics, in turn, can be used to optimize production, compare devices, or predict the output power under different illumination conditions. Equivalent circuit models are the most common model types utilized. Although these models and the estimation of their parameters are thoroughly investigated, little is known about their performance under indoor illumination conditions. This, however, is essential for applications where photovoltaic devices are used indoors, such as for PV-powered sensors, wearables or Internet of Things devices. In this paper, a comprehensive and quantitative study of parameter estimation methods for the two-diode model is conducted, focusing particularly on the performance at indoor illumination levels. We reviewed and implemented a set of six common parameter estimation methods, and evaluate the performance of the estimated parameters on a typical photovoltaic module utilized in indoor scenarios. The results of this investigation demonstrate that there is a large performance variation between different parameter estimation methods, and that many methods have difficulties to estimate accurate parameters at low illumination conditions. Moreover, the majority of methods result in physically infeasible parameters, at least under some of the evaluated conditions. When applying physically motivated parameter scaling methods to these parameters, large estimation errors are observed, which limits the model's applicability for power estimation purposes.

INDEX TERMS Indoor photovoltaics, energy harvesting, photovoltaic cell models, two-diode model, parameter estimation.

I. INTRODUCTION

Energy harvesting facilitates the possibility to implement self-powered electronic systems, such as wireless sensors and IoT edge devices [1]–[4]. These devices can utilize different ambient energy sources, including vibrations, temperature gradients, and ambient light. Among these sources, ambient light is an attractive alternative due to the technological maturity of photovoltaic (PV) transducers, and the general availability of ambient light in many application scenarios [5]. However, ambient light conditions, including their spectra and intensities, differ significantly from each other in outdoor and indoor environments. Outdoor applications are dominated by sunlight, whereas ambient light in indoor applications often originates from artificial light sources with much lower intensities than those observed outdoors [6]–[9].

The associate editor coordinating the review of this manuscript and approving it for publication was Yue Zhang^{ID}.

The scope of this paper lies within artificially illuminated indoor environments.

In order to estimate the available energy in an energy harvesting system prior to its deployment, accurate models are needed. For ambient light energy harvesting, this requires as a first step an accurate model of the PV panel to estimate its electrical output under different illumination conditions [10]–[12]. Different models for this purpose have been suggested, with the most commonly used models being the one-diode and two-diode models. These models are based on electrical equivalent circuit representations that include key device properties, such as the photo current, pn-junction behavior, and resistive losses as lumped circuit elements [13]. To fit the models to a particular PV device, the model parameters are typically extracted from experimental measurements and/or data provided by the manufacturer. To adjust the extracted parameters to other operating conditions, moreover, parameter scaling methods are being used [11], [14]–[16].

Although extensive research efforts have been conducted on the modeling of PV cells and parameter estimation techniques, the existing research focuses to a large extent on outdoor conditions [17]–[25]. As a result, the performance of models, parameter estimation and parameter scaling are typically only evaluated for the solar spectrum (i.e. commonly AM1.5), and high irradiation levels. In contrast, evaluations under indoor illumination conditions are much more limited. In an earlier study, we have evaluated the performance of the one-diode model and a set of commonly used parameter estimation and scaling methods under indoor conditions [26]. This study has demonstrated that most estimation methods can result in model parameters that accurately capture the device's I-V characteristic at the illumination level that the estimation has been performed at, but that these parameters in the majority of cases do not scale well to other illuminations levels. In cases where the resulting models are used for the estimation of output power in different illumination scenarios, this is a major limitation.

The two-diode model has been identified as being superior at low illumination levels as compared to the one-diode model [27]. The main reason for this is its second diode that can take the recombination losses within the depletion region into account. The enhanced performance of the two-diode model is commonly agreed upon in the scientific literature. However, studies conducted in indoor scenarios (i.e. with very low illumination levels) show mixed results leading to conflicting conclusions. In [11], for example, Tinsley *et al.* have demonstrated a direct comparison of the one-diode and two-diode models superiority of the two-diode model, whereas in [28], the authors found the one-diode model to perform better.

Consequently, in this paper we investigate the two-diode model through a systematic review and comparison of different parameter estimation methods, as well as their effects on the model performance under indoor illumination conditions. A set of six (6) parameter estimation methods has been selected from the literature based on their popularity, performances reported in earlier comparisons, and the approach utilized. The methods were implemented and applied to a common indoor PV panel of the same type as in [26], in order to evaluate the performance of the modeled I-V curves, variations in model parameters, and effects of parameter scaling.

With this, the main contributions of this article can be summarized as follows: (i) the evaluation of the two-diode model with its extracted parameters at indoor illumination levels provides a comparison between the model's performance under indoor and outdoor conditions; (ii) the application of different parameter estimation methods provides a quantitative and qualitative comparison of these methods; and (iii) the utilization of the same materials and methods as in [26] enables a direct comparison between one-diode and two-diode model at indoor illumination conditions.

The remainder of this article is structured in the following manner. Section II provides an analysis of related works.

Section III summarizes the fundamental concepts related to the two-diode model. In Section IV, we describe the selected parameter estimation methods. Section V provides information on the data acquisition, the data sets, the implementation of estimation methods, and how the evaluations have been conducted. Section VI presents the results, which is followed by discussions and conclusions in Section VII.

II. RELATED WORK

Due to the importance of accurate PV device modeling and the complex nature of the diode-based models, parameter estimation has been, and continues to be, a highly active research area. Consequently, different parameter estimation methods were introduced in the literature. Several reviews of these methods have been performed, of which the most recent reviews, which include methods for the two-diode model, are those provided in [17]–[19], [21], [23]–[25]. The majority of these reviews are qualitative in nature and group the parameter estimation methods into classes. A common approach is to separate the methods into *analytical* approaches and *meta-heuristic* approaches [17], [24], [25]. Analytical approaches are commonly based on physical reasoning and often include some simplifications. In contrast, meta-heuristic approaches treat the parameter estimation as a non-linear optimization problem, utilizing algorithms such as Particle Swarm Optimization [29], Differential Evolution [30], or Artificial Neural Networks [31]. The analytical methods are, moreover, commonly subdivided into whether or not they require iterative approaches in order to find feasible model parameters.

Methods have also been classified based on the number of model parameters that they estimate [17], [23], as well as the input data that they require [19]. The number of parameters to be estimated has for example been reduced by assuming certain model parameters to be constant [32]–[34], or by simplifying the underlying model itself [35]. The data required by the parameter estimation methods are, in the best case, limited to manufacturer information (i.e. typically datasheet values such as the remarkable points), whereas many methods require additional data in form of experimental measurements [17], [19]. The latter methods often utilize the error between the I-V or P-V characteristics produced by the model and experiment, to stop parameter iterations when a desired tolerance is achieved.

As the majority of reviews compare methods in a qualitative manner and focus on outdoor applications (i.e. typically high solar irradiance levels), a knowledge gap exists in regards to the performance of the two-diode model under indoor illumination conditions. A few individual works exist that have proposed methods that apply the two-diode model in indoor conditions [11], [28], but their results are conflicting. In order to address this gap, in this work we present the results of a quantitative comparison of a selection of parameter estimation methods for the two-diode models at indoor illumination levels.

III. THE TWO-DIODE MODEL

The two-diode model is a common method to describe the key properties of PV devices. The electrical equivalent circuit of this model is illustrated in Figure 1. The circuit consists of a photosensitive current source, two parallel diodes, a shunt resistance, and a series resistance. Mathematically, the terminal voltage and current of the PV cell can be related as

$$I = I_{pv} - I_{d1} - I_{d2} - \frac{V + R_s I}{R_{sh}}, \quad (1)$$

which with the help of Shockley's diode equation can be described as

$$I = I_{pv} - I_{01} \left[\exp\left(\frac{q(V + R_s I)}{n_1 k T}\right) - 1 \right] - I_{02} \left[\exp\left(\frac{q(V + R_s I)}{n_2 k T}\right) - 1 \right] - \frac{V + R_s I}{R_{sh}}. \quad (2)$$

In this I_{pv} is the photo current, I_{01} and I_{02} are the diodes' saturation currents; n_1 and n_2 are the diodes' ideality factors; q is the electron charge; k is the Boltzmann constant; and T is the p-n junction temperature in Kelvin. Furthermore, R_s and R_{sh} are the series resistance and shunt resistance, respectively. As a simplification of equation (2), the thermal voltage can be defined as

$$V_t = \frac{kT}{q}. \quad (3)$$

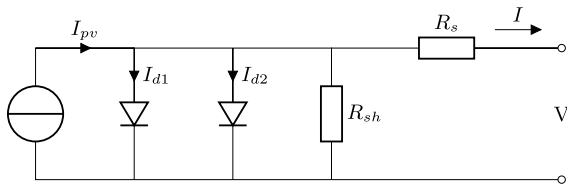


FIGURE 1. Electrical equivalent circuit of the two-diode PV model.

PV devices, moreover, commonly contain multiple PV cells in order to boost output voltage and current through serial and parallel cell connection, respectively. This can be taken into consideration for the model, with

$$I = I_{pv} - I_{01} \left[\exp\left(\frac{V + R_s I}{n_1 N_s V_t}\right) - 1 \right] - I_{02} \left[\exp\left(\frac{V + R_s I}{n_2 N_s V_t}\right) - 1 \right] - \frac{V + R_s I}{R_{sh}}. \quad (4)$$

Herein, N_s denotes the number of PV cells connected in series, and I_{pv} , I_{01} and I_{02} are current values of multiple cells in parallel. R_s and R_{sh} represent resistive losses that result from the device implementation. R_s lumps losses due to contact resistances and non-ideal semiconductors, and R_{sh} represents leakage losses in p-n junctions. In order to achieve a high fill factor, it is desirable for R_s to be small, while R_{sh} is large.

The seven unknown parameters of the two-diode model, I_{pv} , I_{01} , I_{02} , n_1 , n_2 , R_s and R_{sh} , are typically not included by manufacturers in the device datasheet. They therefore

need to be estimated analytically or experimentally. This is commonly referred to as the parameter estimation problem, and as stated earlier different methods can be applied. The hypotheses and approaches of the methods under investigation in this work, are outlined in the following section.

IV. PARAMETER ESTIMATION METHODS

Six parameter estimation methods for the two-diode model have been selected for the comparison in this article. As a consequence of the considerable number of methods proposed in the literature, several criteria have been applied for the method selection. The selected methods are relatively recent (i.e. proposed during the last ten years), and they are based on different approaches and reasoning. Their uptake in the research community (e.g. appearance in review articles), and completeness of information required for reproduction, have also been taken into consideration.

As a results, the methods selected are those proposed by Ishaque *et al.* [34], [36], Maoucha *et al.* [37], Abdulal *et al.* [32], Babu and Gurjar [35], Hejri *et al.* [33], as well as Gbadega-Peter and Saha [38]. Each method is briefly described in the following subsections, and key information is summarized in Table 1.

A. METHOD OF ISHAQUE *et al.* (2011)

Ishaque *et al.* [34] propose an iterative approach to estimate the parameters of the two-diode model. This approach can be interpreted as a two-diode adoption of the method proposed by the authors in [39] for the one-diode model. The authors reduce the set of parameters to be identified based on two assumptions. Firstly, they set the parameters for the diodes' ideality to $n_1 = 1$ and $n_2 = 2$, which is a common simplification based on Shockley's diffusion theory [40]. Secondly, they approximate the diodes' saturation currents to be of same value (i.e. $I_{01} = I_{02}$). Consequently, they reduce the seven unknowns of equation (2) to four unknowns, namely I_{pv} , I_0 , R_s , and R_{sh} .

This reduced set of parameters is estimated based on the following approach. The photo current is estimated with

$$I_{pv} = (I_{sc_STC} + K_i \Delta T) \frac{G}{G_{STC}}, \quad (5)$$

where I_{sc_STC} is the short-circuit current at standard test conditions (STC); K_i is the short-circuit temperature coefficient; and G and G_{STC} are the solar irradiance and solar irradiance at STC, respectively.

The saturation currents are estimated based on

$$I_{01} = I_{02} = \frac{(I_{sc_STC} + K_i \Delta T)}{\exp[(V_{oc_STC} + K_v \Delta T)/V_t] - 1}, \quad (6)$$

with V_{oc_STC} being the open circuit voltage at STC, and K_v the open-circuit temperature coefficient.

Finally, R_s and R_{sh} are obtained through iteration and comparison of the estimated maximum power with the true maximum power. R_s is initialized with zero, and R_{sh} with

$$R_{sh0} = \frac{V_{mp}}{I_{sc} - I_{mp}} - \frac{V_{oc} - V_{mp}}{I_{mp}}. \quad (7)$$

TABLE 1. Overview of two-diode parameter estimation methods.

Method	Year	Method	Assumed parameters	Estimated parameters	Required input ¹
Ishaque	2011	Minimize P_{mp} error	n_1, n_2	I_{pv}, I_0, R_s, R_{sh}	R_s range, P_{mp} tol.
Maoucha	2012	Solve system of nonlinear equations	(n_1, n_2)	$I_{pv}, I_{01}, I_{02}, R_s, R_{sh}$	$V(0.3V_{oc}), I(0.3V_{oc}), V(0.9V_{oc}), I(0.9V_{oc}),$ n_1 range, n_2 range
Abdul Babu	2014	Minimize FF error	n_1	$n_2, I_{pv}, I_0, R_s, R_{sh}$	I-V curve, n_2 range, FF tol.
Hejri	2014	Minimize P_{mp} error	-	$n_1, n_2, I_{pv}, I_{01}, I_{02}$	n_1 range, P_{mp} tol.
Hejri	2014	Solve system of nonlinear equations	n_1, n_2	$I_{pv}, I_{01}, I_{02}, R_s, R_{sh}$	R_s range, tol.
Gbadega-Peter	2019	Minimize P_{mp} and I_{mp} error	-	$n_1, n_2, I_{pv}, I_{01}, I_{02}, R_s, R_{sh}$	R_s range, n_1 range, P_{mp} tol., I_{mp} tol.

V_{mp} and I_{mp} are the voltage and current at the maximum power point (MPP), respectively. With the initial conditions of R_s and R_{sh} defined, R_s is increased on each iteration, and R_{sh} is calculated, such that

$$R_{sh} = \frac{V_{mp}(V_{mp} + I_{mp}R_s)}{V_{mp}\{I_{pv} - A - B\} - V_{mp}I_{mp}}, \quad (8)$$

with

$$A = I_{01}[\exp\left(\frac{V + IR_s}{n_1 V_t}\right) - 1], \quad (9)$$

$$B = I_{02}[\exp\left(\frac{V + IR_s}{n_2 V_t}\right) - 1]. \quad (10)$$

The iterative loop is stopped once the MPP error has fallen below a predefined tolerance value.

B. METHOD OF MAOUCHA *et al.* (2012)

Maoucha *et al.* [37] introduce a parameter estimation method based on a measured I-V curve. Similarly to [34], the seven model parameters are reduced to five by assuming the diodes' ideality factors to be constant (i.e. $n_1 = 1$ and $n_2 = 2$). The remaining five parameters are obtained by solving an equation system of five equations. In order to define this equation system, the authors suggest five representative points of the I-V curve to be extracted with

- $(V_1, I_1) = (0, I_{sc})$ short-circuit point
- $(V_2, I_2) = (0.3V_{oc}, I[0.3V_{oc}])$ V and I at 30% of V_{oc}
- $(V_3, I_3) = (V_{mp}, I_{mp})$ maximum power point
- $(V_4, I_4) = (0.9V_{oc}, I[0.9V_{oc}])$ V and I at 90% of V_{oc}
- $(V_5, I_5) = (V_{oc}, 0)$ open-circuit point

The resulting equation system is given in [37, Eq.(3)], and is proposed by the authors to be solved based on the Trust-Region Method. The following initialization values are suggested by the authors

$$[I_{01}, I_{02}, n_1, n_2, I_{pv}, R_s, R_{sh}] = [10^{-14}, 10^{-11}, 1, 2, 10^{-3}, 2, 50]$$

In order to further improve the obtained parameters, Maoucha *et al.* propose to evaluate the method with different values for the diodes' ideality factors. Value ranges of ($1 \leq n_1 \leq 5$) and ($2 \leq n_2 \leq 7$) are suggested.

C. METHOD OF ABDUL *et al.* (2014)

In [32], Abdulal *et al.* propose an estimation method for the two-diode model parameters based on a graphical approach. The method is similar to the estimation methods for one-diode model parameters proposed by Phang *et al.* [41] and De Blas *et al.* [42], obtaining estimates of R_s and R_{sh} based on the reciprocal slopes of the I-V curves at short-circuit and open-circuit conditions. The resistance values are thus estimated as

$$R_s = R_{s0} = -\left(\frac{dV}{dI}\right)\Bigg|_{V=V_{oc}} \quad (11)$$

$$R_{sh} = R_{sh0} = -\left(\frac{dV}{dI}\right)\Bigg|_{I=I_{sc}} \quad (12)$$

Moreover, I_{pv}, I_{01} and I_{02} are obtained in the same manner as proposed by Ishaque *et al.*, simplifying the saturation currents of both diodes to be of same value. These values can thus be estimated using equations (5) and (6).

Once these values have been obtained, the diodes' ideality factors are estimated following an iterative approach. With n_1 fixed to 1, n_2 is initialized to 1 and increased by 0.1 on each iteration. In each iteration of n_2 , equation (2) is numerically solved and its corresponding fill factor (FF) is calculated according to

$$FF = \frac{V_{mp}I_{mp}}{V_{oc}I_{sc}} \quad (13)$$

The difference between the calculated FF and the expected FF (obtained through measurement or reported by the manufacturer) is used as a metric to evaluate the current n_2 value. The iteration is stopped once the FF error falls below a predefined threshold.

D. METHOD OF BABU AND GURJAR (2014)

In [35], the authors propose a parameter estimation method based on a simplification of the two-diode model presented in Figure 1. In order to simplify the model and reduce the number of parameters to be estimated, the authors remove the resistors R_s and R_{sh} . As such, the parameter estimation problem is reduced to a set of five parameters, namely $I_{pv}, I_{01}, I_{02}, n_1$ and n_2 .

Similarly to others, the authors propose to estimate I_{pv} based on equation (5), and I_{01} is estimated according to

$$I_{01} = \frac{(I_{sc} + K_i \Delta T)}{\exp[(V_{oc} + K_v \Delta T) \cdot q / (N_s k T n_1)] - 1}. \quad (14)$$

The saturation current of the second diode I_{02} is estimated based on a fixed relationship with I_{01} , such that

$$I_{02} = \left(\frac{T^{\frac{2}{5}}}{3.77} \right) I_{01}. \quad (15)$$

This relationship between I_{01} and I_{02} originates in itself from [43].

Finally, the authors utilize an iterative approach to find appropriate solutions for n_1 and n_2 . n_1 is initialized to 1 and incremented on every iteration. For each n_1 a corresponding n_2 is determined, such that

$$n_2 = \frac{qV_{oc}}{N_s T k \ln \left(\frac{I_{pv} - I_{01} (\exp(qV / (N_s k n_1 T)) - 1)}{I_{02}} + 1 \right)}. \quad (16)$$

With all parameters estimated, the I-V equation is numerically solved for a voltage range between 0 and V_{oc} . The estimated current at the MPP is compared to the expected current, and the iteration is ended when a sufficiently small error is achieved.

E. METHOD OF HEJRI et al. (2014)

Hejri et al. [33] propose a mixed analytical-numerical method in order to estimate the parameters of the two-diode model. The set of parameters is reduced, by calculating I_{pv} according to equation (5), and approximating $n_1 = 1$ and $n_2 = 2$. The remaining parameters are determined numerically, by solving the following set of equations

$$\begin{aligned} \frac{I_{mp}}{V_{mp}} &= \frac{I_{01}}{N_s V_t} \left(1 - R_s \frac{I_{mp}}{V_{mp}} \right) \exp \left(\frac{V_{mp} + R_s I_{mp}}{N_s V_t} \right) \\ &+ \frac{I_{02}}{2N_s V_t} \times \left(1 - R_s \frac{I_{mp}}{V_{mp}} \right) \exp \left(\frac{V_{mp} + R_s I_{mp}}{2N_s V_t} \right) \\ &+ \frac{1}{R_{sh}} \left(1 - R_s \frac{I_{mp}}{V_{mp}} \right) \end{aligned} \quad (17)$$

$$\begin{aligned} I_{sc} &= I_{01} \left[\exp \left(\frac{V_{oc}}{N_s V_t} \right) - \exp \left(\frac{R_s I_{sc}}{N_s V_t} \right) \right] \\ &+ I_{02} \left[\exp \left(\frac{V_{oc}}{2N_s V_t} \right) - \exp \left(\frac{R_s I_{sc}}{2N_s V_t} \right) \right] + \frac{V_{oc} - R_s I_{sc}}{R_{sh}} \end{aligned} \quad (18)$$

$$\begin{aligned} &I_{mp} \left(1 + \frac{R_s}{R_{sh}} \right) \\ &= I_{01} \left[\exp \left(\frac{V_{oc}}{N_s V_t} \right) \right. \\ &\quad \left. - \exp \left(\frac{V_{mp} + R_s I_{mp}}{N_s V_t} \right) \right] + I_{02} \left[\exp \left(\frac{V_{oc}}{2N_s V_t} \right) \right. \\ &\quad \left. - \exp \left(\frac{V_{mp} + R_s I_{mp}}{2N_s V_t} \right) \right] + \frac{V_{oc} - V_{mp}}{R_{sh}} \\ &(R_{sh} - R_s) \left[\frac{1}{R_{sh}} + \frac{I_{01}}{N_s V_t} \exp \left(\frac{R_s I_{sc}}{N_s V_t} \right) \right] \end{aligned} \quad (19)$$

$$+ \frac{I_{02}}{2N_s V_t} \exp \left(\frac{R_s I_{sc}}{2N_s V_t} \right) \Big] - 1 = 0 \quad (20)$$

In order to find suitable initial values for the numerical solution of this equation system, the authors propose an analytical approach based on a number of assumptions. Firstly, they analytically solve R_s based on the first-, second- and third-order approximation of the term $\exp(kR_s)$ [33, Eq. (25)]. They then estimate I_{01} and I_{02} based on the simplifications

$$I_{01} = \frac{I_{sc} \exp \left(-\frac{V_{oc}}{2N_s V_t} \right) - (I_{sc} - I_{mp}) \exp \left(-\frac{V_{mp} + R_s I_{mp}}{2N_s V_t} \right)}{\exp \left(\frac{V_{oc}}{2N_s V_t} \right) - \exp \left(\frac{V_{mp} + R_s I_{mp}}{2N_s V_t} \right)} \quad (21)$$

$$I_{02} = \frac{I_{sc} \exp \left(-\frac{V_{oc}}{N_s V_t} \right) - (I_{sc} - I_{mp}) \exp \left(-\frac{V_{mp} + R_s I_{mp}}{N_s V_t} \right)}{\exp \left(-\frac{V_{oc}}{2N_s V_t} \right) - \exp \left(-\frac{V_{mp} + R_s I_{mp}}{2N_s V_t} \right)} \quad (22)$$

Finally, an initial value of R_{sh} is estimated with

$$R_{sh} = \sqrt{\frac{R_s}{\frac{I_{01}}{N_s V_t} \exp \left(\frac{R_s I_{sc}}{N_s V_t} \right) + \frac{I_{02}}{2N_s V_t} \exp \left(\frac{R_s I_{sc}}{2N_s V_t} \right)}} \quad (23)$$

Hejri et al. provide two additional comments on the proposed method. On the one hand, equations (17)–(20) do not always converge, which can be handled by a further simplification that removes I_{01} and I_{02} from the equation system. On the other hand, the analytical solution for R_s does not always lead to a reasonable value, in which case the authors recommend to choose $R_s = 0$ as initial value.

F. METHOD OF GBADEGA-PETER AND SAHA (2019)

In [38], the authors propose a method that combines the methods of Ishaque et al. [34] and Babu and Gurjar [35]. First, I_{pv} , I_{01} and I_{02} are estimated following equations (5), (14) and (15), respectively.

Afterwards two nested iterative loops are created to estimate suitable values for n_1 and n_2 (following the method in [35]), as well as R_s and R_{sh} (following the method in [34]). For this, n_1 and R_s are initiated and the corresponding values for R_{sh} and n_2 are calculated according to equations (16) and (8), respectively.

For each iteration of n_1 , R_s and thus R_{sh} is iterated until the power estimation error at MPP has been reduced to a predefined tolerance. Moreover, n_1 (and consequently n_2) is iterated until the current estimation error at MPP reaches a predefined tolerance as well.

V. IMPLEMENTATION AND EVALUATION APPROACH

The quantitative evaluation of the previously presented parameter estimation methods follows an approach highly

¹Required inputs in addition to the remarkable points, which are required by all methods.

similar to the one presented in [26]. Each parameter estimation method is implemented and applied to I-V datasets of the same PV panel. The resulting parameters are inserted into the two-diode model, which then is used to estimate the I-V characteristics of the PV panel at different illumination conditions. Finally, the estimated I-V characteristics are evaluated against the experimentally obtained datasets in order to quantitatively measure the model performance.

In the following subsections, each step in this process is described in further detail. This description includes the content and acquisition of the datasets, details on method implementations, as well as evaluation metrics used.

A. PV PANEL DATASETS

For the evaluation of the power estimation methods, an IXYS SLMD600H10L PV module has been used, representing a typical PV panel for indoor applications. This panel contains 10 PV cells of monocrystalline silicon, which are connected in series, resulting in a size of $22 \times 35 \text{ mm}^2$. Essential information, such as its remarkable points, are provided by the manufacturer in the device datasheet [44].

Two I-V curve datasets, obtained at different illumination conditions, have been used in this study. The first is a dataset of the PV panel under outdoor illuminations conditions, whereas the other contains I-V characteristics at indoor illumination levels.

The dataset for outdoor conditions has been obtained through the PV panel manufacturer, which limits the information of the exact experimental setup for data generation. However, it is known that a production-grade solar simulator was utilized. The dataset consists of I-V curve measurements at STC (1000 W and 25 °C), and at approximately 200 W and 25 °C. This dataset is mainly used to include a reference for parameter estimation at high solar irradiance levels, as most parameter estimation methods have been created under this condition (i.e. STC).

The main dataset in this study is the one at indoor illumination conditions. This dataset has been experimentally generated for the SLMD600H10L PV panel. The PV panel was during these experiments illuminated by a warm LED lamp (8 W, 2700 K). Typical indoor illumination levels in the range from 100 lx to 1000 lx were generated [45]–[47]. In order to minimize changes to the light spectrum, the different illumination levels were achieved by adjustments to the distance between light source and PV panel, rather than dimming the light source. An AMS TSL2561 ambient light sensor was used to verify the intended illumination condition.

For the measurement of the PV panel's I-V characteristics, a Keysight B2901A source/measure unit (SMU) was used, sweeping the voltage with a 3 mV step-size. The temperature of the panel was maintained at 25 °C through active cooling.

B. METHOD IMPLEMENTATIONS

The previously presented parameter estimation methods were implemented as MATLAB[®] functions. Each function uses input data (e.g. remarkable points) as a parameter list, and

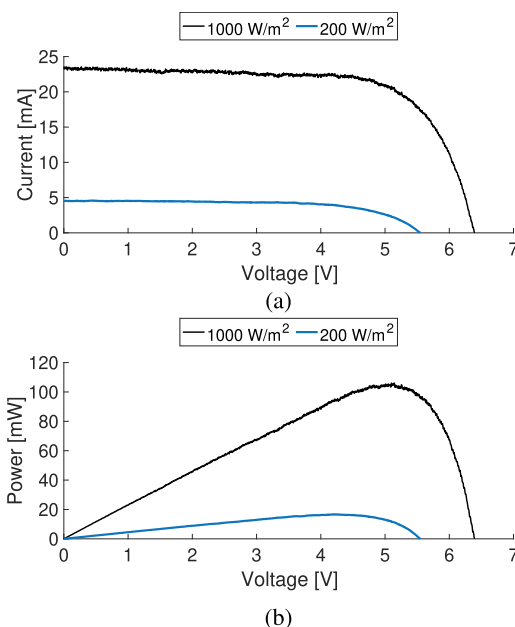


FIGURE 2. IXYS SLMD600H10L PV panel response to outdoor irradiance conditions (25 °C). (a) Resulting I-V characteristics; (b) Resulting P-V characteristics.

produces a set of the seven two-diode model parameter estimates, namely n_1 , n_2 , I_{pv} , I_{01} , I_{02} , R_s and R_{sh} . The description of each method in the literature, was followed as closely as possible. However, some assumptions and implementation decisions had to be made. These are briefly described in the following paragraphs below.

1) NUMERICAL SOLVERS

A subset of the methods include non-linear equations that need to be solved numerically. However, not all methods recommend the same numerical solver to be used. Maoucha *et al.* [37] prescribe to solve their equation system based on the Trusted-Region-Method, whereas in [33] the authors propose to utilize the Newton-Raphson method.

Once the model parameters have been estimated, all evaluated methods require the numerical solution of equation (4) to estimate the I-V characteristic of the PV panel. In order to treat all estimated parameters in the same manner, in all cases the default numerical solver for non-linear equations *fsolve* was used in MATLAB[®].

2) PARAMETER ASSUMPTIONS

The two-diode model requires the identification of seven model parameters. Most parameter estimation methods reduce this set of parameters to simplify the parameter estimation. A typical approach utilized by many methods, for example, is to simplify the ideality factors, such that $n_1 = 1$ and $n_2 = 2$. Such assumptions are commonly well-defined in the description of the respective methods.

In contrast, most methods introduce additional parameters (or conditions) that need to be defined for the implementation.

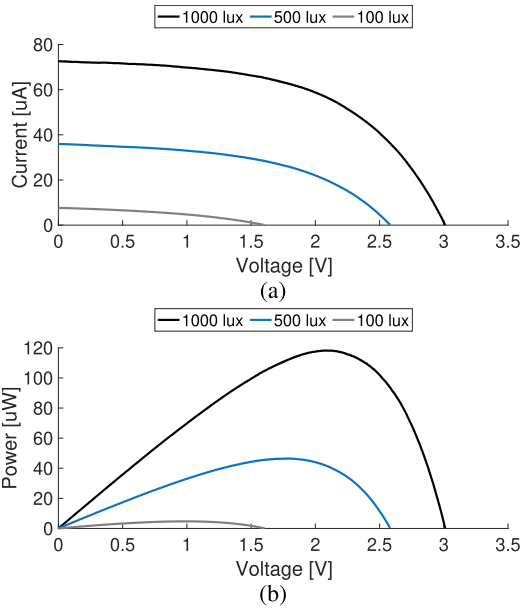


FIGURE 3. IXYS SLMD600H10L PV panel response to indoor illumination conditions (25 °C). (a) Resulting I-V characteristics; (b) Resulting P-V characteristics.

A typical example are the start values, increments, and stop conditions of iterative approaches. These values are often not clearly defined, and might depend to some degree on the underlying PV technology and the scale of the device to be modeled (e.g. acceptable tolerances). Consequently, their determination requires some trial-and-error, which might not always lead to the true optimum. However, the effect of this deviation from the true optimum typically has a low effect.

Other values can be obtained more systematically, such as R_{s0} , R_{sh0} in [32]. For these values, the reciprocal slopes of the I-V curve at $(V_{oc}, 0)$ and $(0, I_{sc})$ are utilized. Similar approaches have previously been used by Celik and Acikgoz [48] and De Blas *et al.* [42]. The estimation accuracy of these values, however, can depend on the resolution and quality of the underlying I-V curve measurements. In this work, we estimated R_{s0} and R_{sh0} such that

$$R_{s0} = \frac{V_k - V_{oc}}{I_k} \tag{24}$$

$$R_{sh0} = \frac{V_j}{I_{sc} - I_j} \tag{25}$$

where (I_j, V_j) and (I_k, V_k) are the j th and k th point on the I-V curve, respectively. For j , typically the first index after $(I_{sc}, 0)$ is selected, whereas for k the last index before $(0, V_{oc})$ is a common choice. In order to reduce the impact of noisy measurement data, multiple slopes with different values for j and k , can be averaged. For our study, m slopes have been used, where m is selected to minimize the RMS error of the estimated parameters.

3) PARAMETER SCALING

In order to be able to estimate I-V characteristics at other environmental conditions than those the PV model parameters

have been estimated for, parameter scaling is required. This means that the parameter dependency on the illumination level and the ambient temperature is taken into consideration. For PV panels illuminated by artificial indoor light sources, temperature effects can typically be neglected [49]. This reduces the parameter scaling to the consideration of illumination level dependency.

Different parameter dependencies to the illumination level have been proposed in the literature. Methods range from those that only assume the photo current I_{pv} to scale with illumination [36], to those that assume a dependency for all parameters [14]. A frequently applied method is the one proposed in [15]. In this method, the photo current increases linearly with illumination level, whereas shunt resistance decreases linearly with illumination level. These two parameters can thus determined according to

$$I_{pv} = \frac{G}{G_{ref}} I_{pv,ref} \tag{26}$$

$$R_{sh} = \frac{G_{ref}}{G} R_{sh,ref} \tag{27}$$

where $I_{pv,ref}$ and $R_{sh,ref}$ are the photo current and shunt resistance at the reference irradiance G_{ref} , respectively. The other model parameters remain constant under changing illumination.

This method is applied to evaluate the scalability of the estimated parameters for all methods investigated in this work.

C. PERFORMANCE METRICS

For a quantitative evaluation of the models that result from the different parameter estimation methods, performance metrics need to be defined. A number of different metrics are being used in the literature with a detailed summary being available in [17].

For this study, the root mean squared error (RMSE) and the normalized root mean squared error (NRMSE) were selected. The RMSE provides an absolute error value in the unit of the model output (i.e. electrical current). In contrast, the NRMSE provides a relative error value, for which we in this case have chosen to normalize the RMSE error with the short circuit current I_{sc} . The NRMSE thus enables a comparison of errors under different conditions (i.e. different scales). The two metrics are calculated such that

$$RMSE = \sqrt{\frac{1}{l} \sum_{x=1}^l (I_{m,x} - I_{e,x})^2}, \tag{28}$$

$$NRMSE = \frac{RMSE}{I_{sc}} \cdot 100\%. \tag{29}$$

Here $I_{m,x}$ and $I_{e,x}$ denote each current value of the model and experiment in the dataset of common length l , respectively.

VI. RESULTS

In this section, we present and discuss the results of the quantitative evaluation that has been performed. The obtained

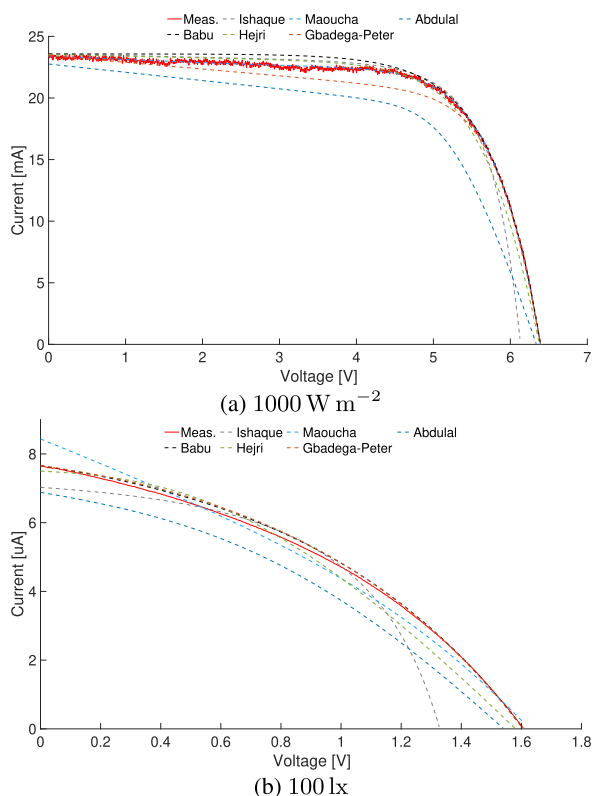


FIGURE 4. Comparison of estimated I-V curves at (a) 1000 W/m² and (b) 100 lx. The measured I-V characteristics (red, solid curve) is provided as reference.

results are the basis for a comparison between the parameter estimation methods for the two-diode model, as well as between the two-diode model and the one-diode model in general. The key results are given in Figures 4, 5 and 6, and Tables 2, 3 and 4. The results contain quantitative data on parameter estimation under different reference conditions (Figure 4 and Tables 2, 3, 4), as well as parameter scaling to different illumination levels (Figures 5 and 6).

A. RESULTS FOR PARAMETER ESTIMATION

The two-diode model parameters that have been estimated by each of the previously described methods are listed in Tables 2 and 3. Table 2 provides the results of parameter estimation at two outdoor irradiance levels (i.e. 1000 W m⁻² and 200 W m⁻²), whereas Table 3 provides the results for two indoor illumination levels (i.e. 1000 lx and 100 lx). In addition to the estimated parameters, the tables contain the resulting I-V curve errors for each set of parameters, utilizing the metrics defined in Section V.

The results show that there is a large variation in parameter values, and in the resulting errors. The variation in parameter values affects all parameters, except the photo current I_{pv} , which stays in a reasonable margin close to the short circuit current value. In a considerable number of cases, the set of estimated parameters includes physically infeasible parameters, such as negative current or resistor values, or extreme

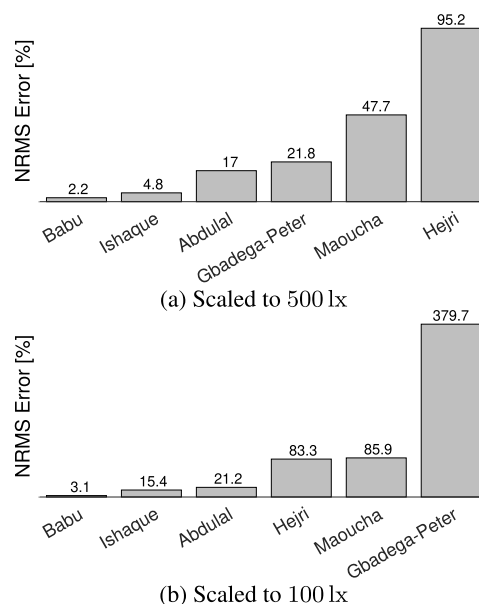


FIGURE 5. Effects of parameter scaling on estimation performance. Parameters, estimated at 1000 lx, are scaled to (a) 500 lx and (b) 100 lx, respectively.

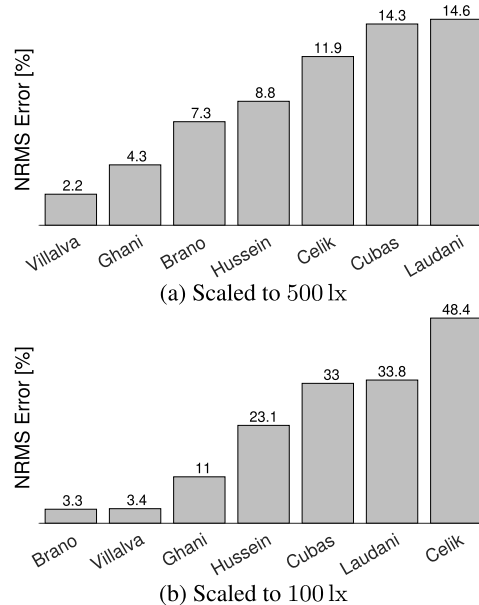


FIGURE 6. Parameter scaling effects on the one-diode models' NRMSE. Parameters, estimated at 1000 lx, are scaled to (a) 500 lx and (b) 100 lx, respectively.

idealty factors. Actually, every method resulted in such infeasible parameters in at least one of the tested illumination conditions. This suggests that the parameters in the individual methods are tweaked for specific error metrics, rather than fulfilling the physical meaning they are assigned. Some general trends can be found in the results, including typically larger R_s and R_{sh} values with decreasing illumination levels. Otherwise, however, the estimated parameters appear to be more random.

TABLE 2. Comparison of the methods' estimated parameters under outdoor conditions.

Method	G [W/m^2]	n_1	n_2	I_{01} [A]	I_{02} [A]	I_{pv} [mA]	R_s [Ω]	R_{sh} [Ω]	RMSE [A]	NRMSE [%]
Ishaque	1000	1	2	3.66e-13	9.26e-8	23.40	-1.55	5214.1	1.10e-3	4.66
	200	1	2	1.88e-12	9.20e-8	4.50	-6.33	16978.8	2.20e-4	4.82
Maoucha	1000	3	2.5	-8.45e-6	2.63e-6	23.44	4.00	3372.1	5.10e-5	0.22
	200	3	2.5	-7.02e-7	9.46e-7	4.50	1.73	53905.8	3.29e-5	0.72
Abdulal	1000	1	4.0	3.66e-13	9.26e-8	23.40	41.66	1450.1	2.66e-3	11.27
	200	1	3.1	1.88e-12	9.20e-8	4.50	330	-28842.0	5.60e-4	12.28
Babu	1000	2.4	-1.14e12	7.36e-7	1.91e-6	23.41	-	-	4.43e-4	1.88
	200	2.46	-4.97e12	6.93e-7	1.80e-6	4.50	-	-	5.66e-5	1.24
Hejri	1000	1	2	9.51e-14	6.92e-8	23.6	14.85	7470.7	6.51e-4	2.76
	200	1	2	9.87e-13	4.47e-8	4.60	138.58	21575.8	1.94e-4	4.25
Gbadega-Peter	1000	1.49	1.70	1.24e-9	3.23e-9	23.60	9.90	1814.6	6.65e-4	2.82
	200	1.89	2.19	4.99e-8	1.29e-7	4.60	7.92	6830	1.64e-4	3.60

TABLE 3. Comparison of the methods' estimated parameters under indoor conditions.

Method	E_V [lx]	n_1	n_2	I_{01} [A]	I_{02} [A]	I_{pv} [μ A]	R_s [Ω]	R_{sh} [Ω]	RMSE [A]	NRMSE [%]
Ishaque	1000	1	2	5.92e-10	2.08e-7	72.24	-2060.3	401 895.1	4.25e-6	5.85
	100	1	2	1.48e-8	3.52e-7	6.93	-20000	4.93e7	5.99e-7	7.82
Maoucha	1000	2.5	7	8.04e-7	-6.08e-6	72.69	464.26	238 093.4	1.11e-7	0.15
	100	1.6	2	1.69e-7	-2.46e-7	9.64	35279.5	245 283.2	3.11e-7	4.06
Abdulal	1000	1	23	5.92e-10	2.08e-7	72.60	10700	414000	9.77e-6	13.45
	100	1	300	1.48e-8	5.32e-7	7.66	83600	883000	1.69e-6	22.06
Babu	1000	2.42	2.56e14	5.72e-7	1.48e-6	72.62	-	-	3.25e-7	0.45
	100	2.91	-3.31e15	1.01e-6	2.62e-6	7.66	-	-	9.70e-8	1.27
Hejri	1000	1	2	6.02e-10	-3.58e-9	72.60	9550	1.09e6	3.03e-6	4.17
	100	1	2	2.19e-8	-1.62e-7	7.66	88800	2.09e6	3.43e-7	4.48
Gbadega-Peter	1000	1.78	1.01e-7	2.63e-7	7.26e-5	72.60	9.90	1.35e5	4.32e-6	5.95
	100	3.07	12.94	1.15e-6	2.98e-6	7.66	9.90	-8.69e5	1.26e-7	1.64

The errors of the I-V curves resulting from the estimated parameters also show considerable variation. In the majority of cases, the error remains below 5 % (NRMSE), but some of the methods produce significantly larger errors than that. The method by Abdulal *et al.* [32] for example, results under all conditions in errors larger 10 %. In contrast, the methods by Maoucha *et al.* [37], as well as Babu and Gurjar [35] produce the lowest errors under most conditions. Something that differentiates these two methods from most others is that they allow for the adjustment of both ideality factors. This provides them with a larger degree of freedom to optimize for a small error. The method of Babu and Gurjar [35] is a clear example that this flexibility results in low I-V curve errors, but does not lead to reasonable physical parameters. Particularly, the ideality factor of the second diode in the model obtains extreme values when using this estimation method.

Although the I-V curve errors are for most methods in the same magnitude, the resulting I-V curve shapes differ quite significantly. This is illustrated on the two most extreme conditions (i.e., outdoor: 1000 $W m^{-2}$, indoor: 100 lx) in Figure 4. Interestingly, the curve forms show much more variations for the two-diode methods, as compared to typical

one-diode methods (cf. Figure 4 in [26]). A potential explanation for this is the fact that the two-diode model has a larger number of parameters. This forces most parameter estimation methods to assume constant value for some of the parameters. In many methods, this results in assumed values for n_1 and n_2 , which have a considerable influence on the curve shape.

Table 4 compares the measured and extracted remarkable points for the four light conditions previously analyzed. These results show that the majority of methods lead to I-V curves that quite accurately estimate the V_{oc} and I_{sc} . In contrast, larger estimation errors need to be expected when estimating the maximum power point. The data in Table 4 also demonstrates an increasing error for lower illumination conditions.

B. RESULTS FOR PARAMETER SCALING

When using the model to estimate PV cell output at different illumination conditions – for example for output power estimations – it is common that the model parameters are estimated under a reference condition, before scaling them to novel conditions. Figure 5 depicts the resulting errors for parameters that have been estimated at 1000 lx, and have consecutively been scaled to 500 lx and 100 lx.

TABLE 4. Comparison of the remarkable points extracted from each method’s I-V curve prediction under different illumination conditions.

		Meas.	Abdual		Babu		Hejri		Ishaque		Maoucha		Gbadega-Peter	
			Value	Error	Value	Error	Value	Error	Value	Error	Value	Error	Value	Error
1000 $\frac{W}{m^2}$	V_{oc} [V]	6.393	6.336	0.89 %	6.393	0.00 %	6.368	0.39 %	6.124	4.21 %	6.393	0.00 %	6.393	8.54 %
	V_{mp} [V]	5.143	4.808	6.51 %	5.024	2.31 %	4.982	3.13 %	5.080	1.22 %	5.080	1.22 %	5.171	0.54 %
	I_{sc} [mA]	23.60	22.76	3.56 %	23.41	0.81 %	23.53	0.30 %	23.41	0.81 %	23.41	0.81 %	23.45	0.64 %
	I_{mp} [mA]	20.63	18.55	10.08 %	20.87	1.16 %	20.73	0.48 %	20.60	0.15 %	20.60	0.15 %	19.36	6.16 %
200 $\frac{W}{m^2}$	V_{oc} [V]	5.549	5.549	0.00 %	5.549	0.00 %	5.528	0.38 %	5.270	5.03 %	5.549	0.00 %	5.549	0.00 %
	V_{mp} [V]	4.247	3.602	15.19 %	4.254	0.16 %	4.121	2.97 %	4.290	1.01 %	4.254	0.16 %	4.380	3.13 %
	I_{sc} [mA]	4.56	4.56	0.00 %	4.50	1.32 %	4.53	0.66 %	4.50	1.32 %	4.50	1.32 %	4.55	0.22 %
	I_{mp} [mA]	3.93	4.15	5.60 %	3.92	0.25 %	3.88	1.27 %	3.85	2.04 %	3.88	1.27 %	3.59	8.65 %
1000 lx	V_{oc} [V]	3.011	2.981	1.00 %	3.008	0.10 %	2.998	0.43 %	2.722	9.60 %	3.011	0.00 %	3.011	0.00 %
	V_{mp} [V]	2.080	1.909	8.22 %	2.095	0.72 %	1.954	6.06 %	2.083	0.14 %	2.095	0.72 %	2.191	5.34 %
	I_{sc} [uA]	72.62	70.75	2.58 %	72.62	0.00 %	71.99	0.87 %	72.67	0.07 %	72.78	0.22 %	72.61	0.01 %
	I_{mp} [uA]	56.86	56.09	1.35 %	56.45	0.72 %	59.68	4.96 %	56.77	0.16 %	56.22	1.13 %	48.94	13.93 %
100 lx	V_{oc} [V]	1.606	1.540	4.11 %	1.606	0.00 %	1.579	1.68 %	1.327	17.37 %	1.606	0.00 %	1.607	0.06 %
	V_{mp} [V]	1.006	0.879	12.62 %	0.978	2.78 %	0.885	12.03 %	0.933	7.26 %	0.943	6.26 %	0.975	3.08 %
	I_{sc} [uA]	7.66	6.88	10.18 %	7.66	0.00 %	7.50	2.09 %	7.03	8.22 %	8.44	10.18 %	7.66	0.00 %
	I_{mp} [uA]	4.69	4.37	6.82 %	4.92	4.90 %	5.08	8.32 %	5.13	9.38 %	4.67	0.43 %	4.96	5.76 %

The results show that there is a large variation in the estimation error, even for scaled parameters. Estimation errors range from 2.2 % (Babu, 500 lx) to 379.7 % (Gbadega-Peter, 100 lx). It can also be observed that, for the majority of methods, the estimation error increases when scaling to 100 lx, that means a light condition further away from the reference condition. The parameters performing best when being scaled to other conditions are those estimated with the method by Babu and Gurjar [35]. This method resulted also in parameters with low errors in the parameter estimation. However, high performance in parameter estimation does not automatically lead to parameters that scale well. This is for example demonstrated by the method proposed by Maoucha *et al.* [37]. This method resulted in parameters performing among the best when being estimated for a specific condition, but performed among the worst when being scaled to other conditions.

A potential explanation for the relatively high performance of the parameters estimated by the method of Babu and Gurjar [35], is its simplification to neglect the model resistances. As a result, the model only utilizes one parameter that needs to be scaled with different illumination conditions, namely I_{pv} . All other methods require the scaling of R_{sh} as well. Consequently, Babu and Gurjar’s method does not adjust the I-V curve form with changing illumination, which appears to be beneficial when scaling is performed over a sufficiently small range of conditions.

Figure 6 provides comparable scaling results for commonly used parameter estimation methods of the one-diode model [26]. Similarly to the parameter estimation, the comparison of scaling results demonstrates in general larger estimation errors for the two-diode model than for the one-diode model. A likely explanation for this is the large number of infeasible model parameters that are obtained as a result of the two-diode model parameter estimation methods. With a limited physical meaning of the obtained parameters, their scaling according to physically motivated assumptions makes little sense.

VII. CONCLUSION

Equivalent circuit models and parameter estimation methods for their parameters are being researched intensively. However, little is known about their performance in indoor illumination conditions, and method comparisons are mainly qualitative in nature. In this work, we evaluated parameter estimation methods for the two-diode equivalent circuit model. A selection of six representative methods have been implemented and evaluated quantitatively. The results are presented separately for parameter estimation at specific illumination conditions, and the effect on parameter scaling to other conditions than those initially estimated for.

The results demonstrate that there is a considerable variation in the performance of parameter estimation methods. Although the majority of methods results in acceptable performance of the estimated parameters (< 5 %) at high irradiation, their performance typically degrades with decreasing illumination levels. Only a few methods continue to provide accurate estimations of the I-V curve shape even at low illumination. It was found that these methods allowed for the variation of the diode ideality factors, and thus provided more freedom to alter the curve form of the I-V characteristic. It was moreover found that many estimation methods result in infeasible parameters. Although these parameters may lead to low I-V curve errors – which is a metric they typically optimize for – the resulting parameters have little physical meaning. It can therefore be concluded that a physical interpretation of the estimated parameters, in the majority of cases, is unreasonable.

This has consequences on the scaling of parameters based on physical reasoning. The results of scaling the estimated parameters to illumination conditions other than those they have been estimated at, demonstrate that scaling in the majority of cases leads to significant estimation errors. The only method that maintained acceptable estimation accuracy (< 5 %) was the method proposed by Babu and Gurjar [35]. This method differentiates itself from the others as it utilizes

a simplified two-diode model that neglects resistive losses. This suggests that a simpler model may be more robust in these situations.

This is supported by the comparison of the results with those of typical methods for the one-diode model. Although the performance of the model depends on the individual parameter estimation method utilized, the general trend shows that the one-diode model outperforms the two-diode model under the evaluated conditions. The second diode in the two-diode model is typically associated with a higher performance especially at low illumination conditions. However, in practice the additional parameters of the model require assumptions to enable parameter estimation. The results in this study suggest that the negative effect of these assumptions may outweigh the model's general improved level of detail.

In general, the findings of this study suggest that the two-diode model should be used with care when estimations are to be performed at indoor illumination levels and for PV devices typically used in such conditions. The model performance is extremely sensitive to the parameter estimation method employed, and in principle none of the methods provides performances that clearly motivate a more complex model. The common benefit of diode models to contain physically deduced parameters is challenged by the obtained results. With all investigated parameter estimation methods leading to physically infeasible parameters under some conditions, a question about the purpose of physical models for power estimation is raised.

REFERENCES

- [1] K. S. Adu-Manu, N. Adam, C. Tapparello, H. Ayatollahi, and W. Heinzelman, "Energy-harvesting wireless sensor networks (EH-WSNs): A review," *ACM Trans. Sensor Netw.*, vol. 14, no. 2, pp. 1–50, Jul. 2018.
- [2] S. Cao and J. Li, "A survey on ambient energy sources and harvesting methods for structural health monitoring applications," *Adv. Mech. Eng.*, vol. 9, no. 4, Apr. 2017, Art. no. 168781401769621.
- [3] Y. Ramadass, "Powering the Internet of Things," in *Proc. IEEE Hot Chips 26 Symp. (HCS)*, Aug. 2014, pp. 375–380.
- [4] F. K. Shaikh and S. Zeadally, "Energy harvesting in wireless sensor networks: A comprehensive review," *Renew. Sustain. Energy Rev.*, vol. 55, pp. 1041–1054, Mar. 2016.
- [5] G. Apostolou, A. Reinders, and M. Verwaal, "Comparison of the indoor performance of 12 commercial PV products by a simple model," *Energy Sci. Eng.*, vol. 4, no. 1, pp. 69–85, Jan. 2016.
- [6] Y. Afsar, J. Sarik, M. Gorlatova, G. Zussman, and I. Kymissis, "Evaluating photovoltaic performance indoors," in *Proc. 38th IEEE Photovoltaic Spec. Conf.*, Jun. 2012, pp. 1948–1951.
- [7] J. F. Randall and J. Jacot, "Is AM1.5 applicable in practice? Modelling eight photovoltaic materials with respect to light intensity and two spectra," *Renew. Energy*, vol. 28, no. 12, pp. 1851–1864, Oct. 2003.
- [8] N. H. Reich, W. G. J. H. M. van Sark, and W. C. Turkenburg, "Charge yield potential of indoor-operated solar cells incorporated into product integrated photovoltaic (PIPV)," *Renew. Energy*, vol. 36, no. 2, pp. 642–647, Feb. 2011.
- [9] K. Ruhle, S. W. Glunz, and M. Kasemann, "Towards new design rules for indoor photovoltaic cells," in *Proc. 38th IEEE Photovoltaic Spec. Conf.*, Jun. 2012, pp. 2588–2591.
- [10] X. Ma, S. Bader, and B. Oelmann, "A scalable, data-driven approach for power estimation of photovoltaic devices under indoor conditions," in *Proc. 7th Int. Workshop Energy Harvesting Energy-Neutral Sens. Syst. - ENSys*, 2019, pp. 29–34.
- [11] N. F. Tinsley, S. T. Witts, J. M. R. Ansell, E. Barnes, S. M. Jenkins, D. Raveendran, G. V. Merrett, and A. S. Weddell, "Enspect: A complete tool using modeling and real data to assist the design of energy harvesting systems," in *Proc. 3rd Int. Workshop Energy Harvesting Energy Neutral Sens. Syst. - ENSys*, 2015, pp. 27–32.
- [12] X. Ma, S. Bader, and B. Oelmann, "Power estimation for indoor light energy harvesting systems," *IEEE Trans. Instrum. Meas.*, vol. 69, no. 10, pp. 7513–7521, Oct. 2020.
- [13] M. Wolf and H. Rauschenbach, "Series resistance effects on solar cell measurements," *Adv. Energy Convers.*, vol. 3, no. 2, pp. 455–479, Apr. 1963.
- [14] V. Lo Brano, A. Orioli, G. Ciulla, and A. Di Gangi, "An improved five-parameter model for photovoltaic modules," *Sol. Energy Mater. Sol. Cells*, vol. 94, no. 8, pp. 1358–1370, Aug. 2010.
- [15] W. De Soto, S. A. Klein, and W. A. Beckman, "Improvement and validation of a model for photovoltaic array performance," *Sol. Energy*, vol. 80, no. 1, pp. 78–88, Jan. 2006.
- [16] A. Mermoud and T. Lejeune, "Performance assessment of a simulation model for PV modules of any available technology," in *Proc. 25th Eur. Photovoltaic Sol. Energy Conf.*, 2010, pp. 1–6.
- [17] R. Abbassi, A. Abbassi, M. Jemli, and S. Chebbi, "Identification of unknown parameters of solar cell models: A comprehensive overview of available approaches," *Renew. Sustain. Energy Rev.*, vol. 90, pp. 453–474, Jul. 2018.
- [18] M. Q. Baig, H. A. Khan, and S. M. Ahsan, "Evaluation of solar module equivalent models under real operating conditions—A review," *J. Renew. Sustain. Energy*, vol. 12, no. 1, Jan. 2020, Art. no. 012701.
- [19] V. J. Chin, Z. Salam, and K. Ishaque, "Cell modelling and model parameters estimation techniques for photovoltaic simulator application: A review," *Appl. Energy*, vol. 154, pp. 500–519, Sep. 2015.
- [20] G. Ciulla, V. Lo Brano, V. Di Dio, and G. Cipriani, "A comparison of different one-diode models for the representation of I–V characteristic of a PV cell," *Renew. Sustain. Energy Rev.*, vol. 32, pp. 684–696, Apr. 2014.
- [21] D. T. Cotfas, P. A. Cotfas, and S. Kaplanis, "Methods to determine the DC parameters of solar cells: A critical review," *Renew. Sustain. Energy Rev.*, vol. 28, pp. 588–596, Dec. 2013.
- [22] M. A. Hasan and S. K. Parida, "An overview of solar photovoltaic panel modeling based on analytical and experimental viewpoint," *Renew. Sustain. Energy Rev.*, vol. 60, pp. 75–83, Jul. 2016.
- [23] A. M. Humada, M. Hojabri, S. Mekhilef, and H. M. Hamada, "Solar cell parameters extraction based on single and double-diode models: A review," *Renew. Sustain. Energy Rev.*, vol. 56, pp. 494–509, Apr. 2016.
- [24] A. R. Jordehi, "Parameter estimation of solar photovoltaic (PV) cells: A review," *Renew. Sustain. Energy Rev.*, vol. 61, pp. 354–371, Aug. 2016.
- [25] R. Tamrakar and A. Gupta, "A review extraction of solar cell modelling parameters," *Int. J. Innov. Res. Electr., Electron., Instrum. Control Eng.*, vol. 3, pp. 55–60, Jan. 2015.
- [26] S. Bader, X. Ma, and B. Oelmann, "One-diode photovoltaic model parameters at indoor illumination levels—A comparison," *Sol. Energy*, vol. 180, pp. 707–716, Mar. 2019.
- [27] D. S. H. Chan and J. C. H. Phang, "Analytical methods for the extraction of solar-cell single- and double-diode model parameters from I–V characteristics," *IEEE Trans. Electron Devices*, vol. 34, no. 2, pp. 286–293, Feb. 1987.
- [28] M. Masoudinejad, M. Kamat, J. Emmerich, M. ten Hompel, and S. Sardesai, "A gray box modeling of a photovoltaic cell under low illumination in materials handling application," in *Proc. 3rd Int. Renew. Sustain. Energy Conf. (IRSEC)*, Dec. 2015, pp. 1–6.
- [29] E. Q. B. Macabebe, C. J. Sheppard, and E. E. van Dyk, "Parameter extraction from I–V characteristics of PV devices," *Sol. Energy*, vol. 85, no. 1, pp. 12–18, Jan. 2011.
- [30] K. Ishaque and Z. Salam, "An improved modeling method to determine the model parameters of photovoltaic (PV) modules using differential evolution (DE)," *Sol. Energy*, vol. 85, no. 9, pp. 2349–2359, Sep. 2011.
- [31] M. Karamirad, M. Omid, R. Alimardani, H. Mousazadeh, and S. N. Heidari, "ANN based simulation and experimental verification of analytical four- and five-parameters models of PV modules," *Simul. Model. Pract. Theory*, vol. 34, pp. 86–98, May 2013.
- [32] F. Abdulal, N. Anani, and N. Bowring, "Comparative modelling and parameter extraction of a single- and two-diode model of a solar cell," in *Proc. 9th Int. Symp. Commun. Syst., Netw. Digit. Sign. (CSNDSP)*, Jul. 2014, pp. 856–860.

- [33] M. Hejri, H. Mokhtari, M. R. Azizian, M. Ghandhari, and L. Soder, "On the parameter extraction of a five-parameter double-diode model of photovoltaic cells and modules," *IEEE J. Photovolt.*, vol. 4, no. 3, pp. 915–923, May 2014.
- [34] K. Ishaque, Z. Salam, and H. Taheri, "Simple, fast and accurate two-diode model for photovoltaic modules," *Sol. Energy Mater. Sol. Cells*, vol. 95, no. 2, pp. 586–594, Feb. 2011.
- [35] B. C. Babu and S. Gurjar, "A novel simplified two-diode model of photovoltaic (PV) module," *IEEE J. Photovolt.*, vol. 4, no. 4, pp. 1156–1161, Jul. 2014.
- [36] K. Ishaque, Z. Salam, and H. Taheri, "Accurate MATLAB simulink PV system simulator based on a two-diode model," *J. Power Electron.*, vol. 11, no. 2, pp. 179–187, Mar. 2011.
- [37] A. Maucha, F. Djeflal, D. Arar, N. Lakhdar, T. Bendib, and M. A. Abdi, "An accurate organic solar cell parameters extraction approach based on the illuminated I-V characteristics for double diode modeling," in *Proc. 1st Int. Conf. Renew. Energies Veh. Technol.*, Mar. 2012, pp. 74–77.
- [38] A. Gbadega Peter and A. K. Saha, "Electrical characteristics improvement of photovoltaic modules using two-diode model and its application under mismatch conditions," in *Proc. Southern Afr. Universities Power Eng. Conf./Robotics Mechatronics/Pattern Recognit. Assoc. South Afr. (SAUPEC/RobMech/PRASA)*, Jan. 2019, pp. 328–333.
- [39] M. G. Villalva, J. R. Gazoli, and E. R. Filho, "Comprehensive approach to modeling and simulation of photovoltaic arrays," *IEEE Trans. Power Electron.*, vol. 24, no. 5, pp. 1198–1208, May 2009.
- [40] C.-T. Sah, R. Noyce, and W. Shockley, "Carrier generation and recombination in P-N junctions and P-N junction characteristics," *Proc. IRE*, vol. 45, no. 9, pp. 1228–1243, Sep. 1957.
- [41] J. C. H. Phang, D. S. H. Chan, and J. R. Phillips, "Accurate analytical method for the extraction of solar cell model parameters," *Electron. Lett.*, vol. 20, no. 10, pp. 406–408, May 1984.
- [42] M. A. de Blas, J. L. Torres, E. Prieto, and A. Garcia, "Selecting a suitable model for characterizing photovoltaic devices," *Renew. Energy*, vol. 25, no. 3, pp. 371–380, Mar. 2002.
- [43] S. Gupta, H. Tiwari, M. Fozdar, and V. Chandna, "Development of a two diode model for photovoltaic modules suitable for use in simulation studies," in *Proc. Asia-Pacific Power Energy Eng. Conf.*, Mar. 2012, pp. 1–4.
- [44] *IXOLAR High Efficiency SolarMD*, IXYS Corporation, Milpitas, CA, USA, 2010, Nov. 2016.
- [45] X. Ma, S. Bader, and B. Oelmann, "Characterization of indoor light conditions by light source classification," *IEEE Sensors J.*, vol. 17, no. 12, pp. 3884–3891, Jun. 2017.
- [46] Y. K. Tan and S. K. Panda, "Energy harvesting from hybrid indoor ambient light and thermal energy sources for enhanced performance of wireless sensor nodes," *IEEE Trans. Ind. Electron.*, vol. 58, no. 9, pp. 4424–4435, Sep. 2011.
- [47] W. S. Wang, T. O'Donnell, N. Wang, M. Hayes, B. O'Flynn, and C. O'Mathuna, "Design considerations of sub-mW indoor light energy harvesting for wireless sensor systems," *ACM J. Emerg. Technol. Comput. Syst.*, vol. 6, no. 2, pp. 1–26, Jun. 2010.
- [48] A. N. Celik and N. Acikgoz, "Modelling and experimental verification of the operating current of mono-crystalline photovoltaic modules using four- and five-parameter models," *Appl. Energy*, vol. 84, no. 1, pp. 1–15, Jan. 2007.
- [49] A. Fajardo Jaimes and F. Rangel de Sousa, "Simple modeling of photovoltaic solar cells for indoor harvesting applications," *Sol. Energy*, vol. 157, pp. 792–802, Nov. 2017.



XINYU MA (Student Member, IEEE) received the B.Sc. and M.Sc. degrees in electronics engineering from Mid Sweden University, Sundsvall, Sweden, in 2011 and 2014, respectively, where she is currently pursuing the Ph.D. degree with the Department of Electronics Design. Her research interests include ambient light energy harvesting for wireless sensor networks with research interests in the modeling and characterization of PV systems under artificial lighting conditions.



SEBASTIAN BADER (Senior Member, IEEE) received the Ph.D. degree in electronics from Mid Sweden University, Sundsvall, Sweden, in 2013, and the Dipl.-Ing. degree from the University of Applied Sciences, Wilhelmshaven, Germany. He is currently an Assistant Professor of electronics engineering with the Department of Electronics Design, Mid Sweden University. His research interests include energy harvesting, networked embedded systems, and low-power sensor systems and their applications. His current research interests include energy transducer design, optimization and modeling, as well as the integration and optimization of self-powered sensing systems.



BENGT OELMANN received the Doctor of Technology degree in electronics from the Royal Institute of Technology, Stockholm, Sweden, in 2000. He is currently a Full Professor in electronics system design with Mid Sweden University, Sundsvall, Sweden. His current research interests include low-energy embedded system design, energy harvesting, and embedded sensor technology.